NANO LETTERS

pubs.acs.org/NanoLett

Letter

Patterning on Living Tardigrades

Zhirong Yang, Shan Wu, Kang Zhao, Ding Zhao,* and Min Qiu*

Cite This: *Nano Lett.* 2025, 25, 6168−6175

Read Online

ACCESS | Metrics & More | Article Recommendations | Supporting Information

ABSTRACT: Micro/nanofabrication techniques have revolutionized modern photonics and electronics. However, conventional methods remain incompatible with living organisms due to inherent constraints including nonconformal coating, radiation damage, and toxic solvent requirements. Here, we present ice lithography for direct fabrication of micro/nanoscale patterns on the surfaces of tardigrades in their cryptobiotic state. Remarkably, upon rehydration the tardigrades revive, retaining the patterns on their surfaces. By precisely controlling parameters such as ice thickness, beam energy, and substrate properties, this method minimizes sample damage while achieving patterns as small as 72 nm. These patterns remain stable even after stretching, solvent immersion, rinsing, and drying. This approach provides new insights into tardigrades' resilience and has potential applications in cryopreservation, biomedicine, and astrobiology. Furthermore, integrating micro/nanofabrication techniques with living organisms could catalyze advancements in biosensing, biomimetics, and living microrobotics.

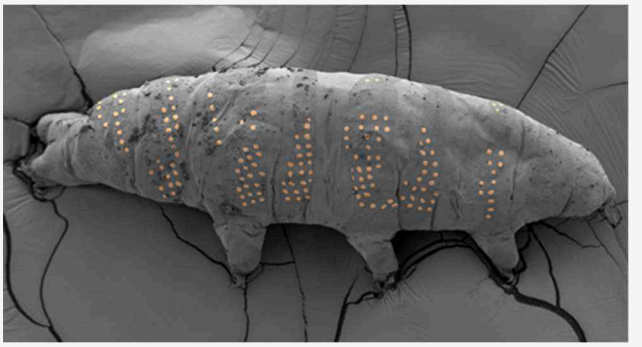

KEYWORDS: *micro/nanofabrication, ice lithography, living organisms, wearables, biosensors*

Micronanoengineers may often look with envy at men like Richard Feynman who predicted a new world on a small scale before the birth of nanotechnology. No one expected that how to write the Encyclopaedia Britannica on the head of a pin, one of Feynman's playful suggestions would coincide with a key driver of modern information industry.[1] Advancements in micro and nanofabrication technologies have enabled the large-scale integration of devices, such as integrated circuits and nanoscale sensors,[2−4] onto planar substrates. Simultaneously, progress in bioelectronics, materials science, and medicine has introduced new challenges for these fabrication techniques. The incorporation of patterns, such as electrodes and circuits, into micro and nanoscale biological systems merges electronics, photonics, and stimuli-responsive materials, offering significant potential for the development of advanced intelligent sensing and control devices.

Considerable efforts have been made to adapt existing methods and develop new approaches that enable compatibility between micro/nanofabrication techniques and delicate biological organisms.[5] Recent advancements, including nanoimprint lithography,[6] 3D printing,[7] self-assembly,[8] and laser printing,[9] have shown promise for micro and nanoscale processing on flexible or fragile substrates. Researchers are also exploring methods such as deposition of force-mediating nanoparticles on cells or 3D bioprinting of composite formulations combining nanomaterials and cells to improve the creation of biological interfaces.[10−12] However, integrating high-resolution patterns onto micro and nanoscale living organisms remains an unsolved challenge. This limitation arises from the incompatibility of many conventional fabrication methods with biological systems, including processes such as etching, high-temperature baking, the use of toxic solvents, electron radiation, and vacuum-based techniques.[5] Furthermore, most fabrication methods are ill-suited to handle irregular surfaces, with the complex and fragile topography of biological surfaces presenting a significant challenge for conventional techniques.

In this study, we integrate semiconductor manufacturing techniques with biology, demonstrating that electron-beam lithography (EBL) can be employed to fabricate micro and nanoscale patterns on extremophilic organisms such as tardigrades. This process must be carried out at cryogenic temperatures in a technique known as ice lithography, an emerging variation of the traditional method. The tardigrade, often called the "water bear," is renowned for its remarkable resilience in its cryptobiotic state,[13] making it an ideal subject for initial experiments. In ice lithography, vaporized chemicals condense onto the sample surface to form conformal electron resists, making this technique particularly suitable for micro/nanofabrication on small, delicate, or non-planar objects.[14,15] A key advantage of using ice as an electron resist is its ability to

Received: January 17, 2025
Revised: March 17, 2025
Accepted: March 18, 2025
Published: April 1, 2025

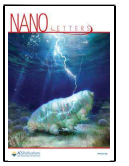

https://doi.org/10.1021/acs.nanolett.5c00378
Nano Lett. 2025, 25, 6168−6175

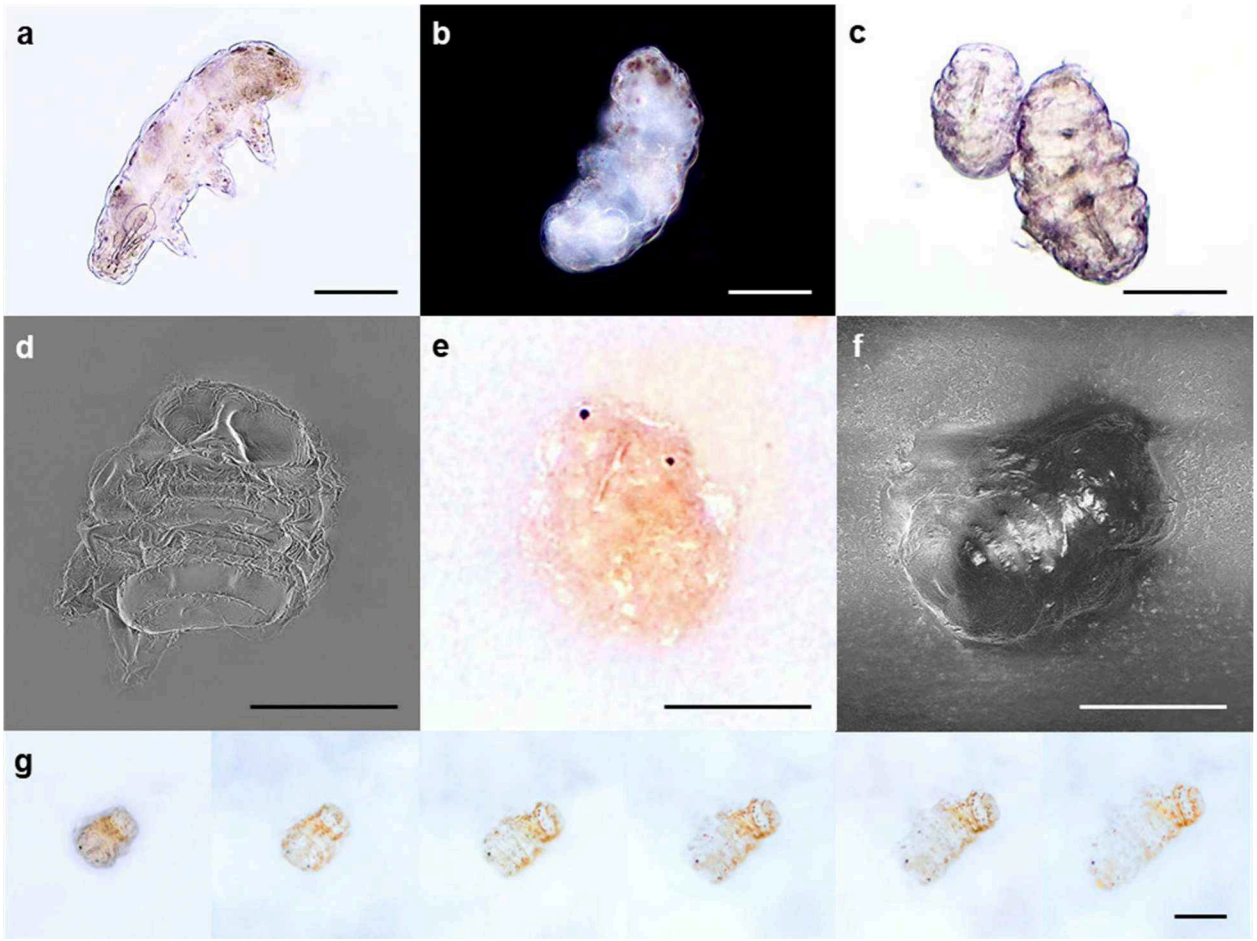

Figure 1. Resilience testing of tardigrades. (a) Optical image and (b) fluorescent image of the extremotolerant tardigrade in a hydrated condition. Optical images (c and e) and SEM images (d and f) of cryptobiotic tardigrades under extreme conditions: desiccation (c), vacuum and electron radiation (d), freezing in liquid nitrogen (e), and covering with solid anisole (f). (g) Revival process from tun state to active state with water. Scale bars: 50 μm.

minimize electron radiation damage to the sample.[16,17] While cryopreservation techniques have advanced significantly, preventing damage caused by ice crystal formation during freezing remains a challenge.[18] Ice lithography circumvents this issue by utilizing ice in its amorphous state, thereby preventing crystal formation and protecting the sample. Using this method, we successfully fabricated in situ micro and nanoscale patterns of arbitrary shapes on living tardigrades, including a line array with a line width of 72 nm. These patterns remained securely attached to the tardigrade's body even after stretching, solvent immersion, rinsing, and drying. The insights gained from this work could advance researchers' ability to detect and manipulate biological entities at the micro and nanoscale, with potential applications in cryopreservation, microbial sensing, and the development of living micro-robotic systems.

In our initial investigation into micro/nanofabrication for biological systems, selecting an appropriate biological species and confirming its viability were critical. The tardigrade, a microscopic aquatic invertebrate, is renowned for its exceptional resilience in its cryptobiotic state, allowing it to endure extreme conditions such as freezing, high pressure, and intense radiation.[19,20] These remarkable traits make tardigrades ideal candidates for our preliminary experiments. In this study, we captured and cultured tardigrades, inducing their transition from an active state (Figures 1a and 1b) to a cryptobiotic state (Figure 1c) under low-humidity conditions. We then thoroughly assessed their resilience under extreme conditions, including exposure to high vacuum and electron radiation in a scanning electron microscope (SEM) (Figure 1d), freezing in liquid nitrogen (Figure 1e), and exposure to solid anisole (Figure 1f). After removal of these extreme conditions, the tardigrades were successfully revived from the cryptobiotic state with water (Figure 1g).

The successful fabrication of intricate micro/nanopatterns is essential for the development of micro/nanodevices. Ice lithography, an emerging micro/nano processing technology, offers significant advantages and holds great promise for applications on the surface of living organisms.[21] By utilizing ice as a resist, it provides unique benefits, including high-precision in situ processing, the ability to handle diverse substrates, and protection against electron radiation. Previous studies have demonstrated it can deal with fragile, irregular, or sensitive materials, such as atomic force microscope (AFM) tips,[14] microfibers,[22] and perovskites.[23] Building on these findings, we employed ice lithography to create precise patterns on tardigrades. The schematic in Figure 2 illustrates the experimental procedure for ice lithography on the tardigrade. The instrumentation and detailed operational procedures have been described previously.[24] Initially, the cryptobiotic tardigrade sample was cooled to <130 K (Figure

https://doi.org/10.1021/acs.nanolett.5c00378
Nano Lett. 2025, 25, 6168−6175

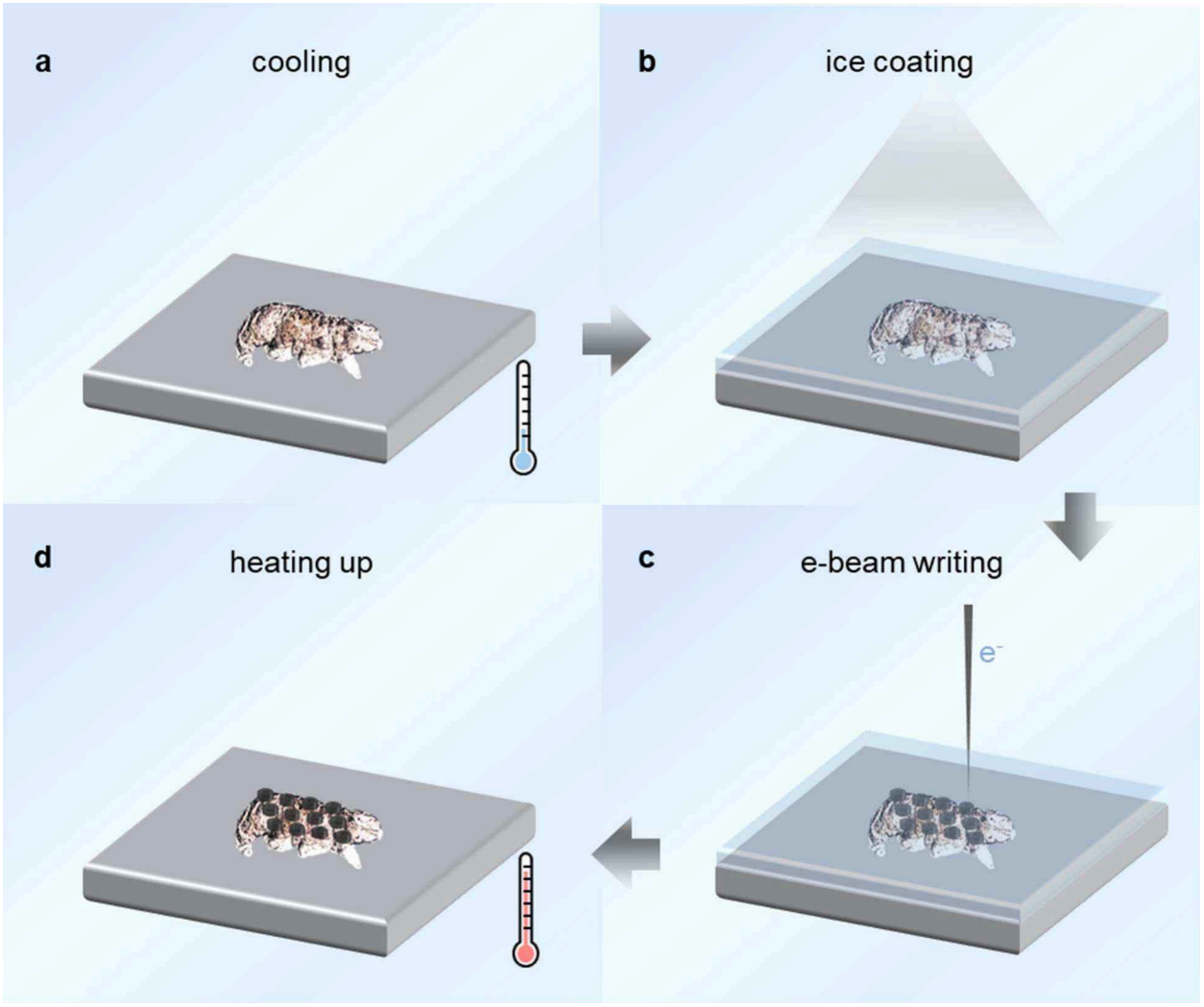

Figure 2. Schematic diagram of ice lithography (IL) for patterning on the tardigrade. (a) The sample is cooled to 130 K using a cold stage. (b) Anisole vapor is deposited onto the sample surface. (c) An electron beam irradiates the solid anisole according to a predetermined pattern. (d) The sample is heated up to room temperature. The nonirradiated anisole sublimes, while the irradiated forms the pattern on the sample.

2a), followed by the condensation of vaporized anisole onto the sample, forming a thin layer of amorphous film (Figure 2b). A focused electron beam then irradiated the film according to the predetermined pattern, locally modifying the chemical composition of the anisole (Figure 2c). During irradiation, oxygen atoms were removed, resulting in a significant increase in the carbon content (weight percentage >94%).[25] This alteration greatly reduced the toxicity of the exposed anisole, enhancing its biocompatibility. The sample was gradually heated to room temperature in a vacuum, causing the unexposed anisole to sublimate and leaving the designed nanostructures directly on the cryptobiotic tardigrade (Figure 2d). Finally, the sample was removed from the SEM chamber, and the tardigrade was rehydrated until it revived.

To ensure the protection of biological samples during e-beam writing, ice thickness and beam energy should be carefully optimized. The radiation resistance of biological samples is inherently limited. While solid anisole helps reduce electron radiation damage, excessive thickness can lead to charge accumulation, which impacts electron beam focusing and observation. In our experiment, we preferred an ice layer with a thickness of less than 200 nm. At the same time, a lower beam energy was beneficial to minimizing charge buildup (Figure S1). Given that tardigrades are carbon-based organisms with chemical compositions similar to the substrate and created patterns, and that their surface morphology is highly uneven, the Secondary Electron (SE) detector proved particularly suitable for capturing high-resolution, three-dimensional structural details (Figure S2). Monte Carlo simulations were performed for electron beams with energies of 1, 2, and 3 keV to assess the energy absorption distribution of anisole at various energy levels, with the results shown in Figure S3. During the simulations, the electron penetration depth was estimated, although it does not directly correspond to the actual thickness of solidified anisole. The results indicated that a 1 keV electron beam has a penetration depth of approximately 38 nm, making it challenging to observe the created pattern under an optical microscope. In contrast, a 3 keV electron beam has a penetration depth exceeding 200 nm, which could cause excessive radiation damage if the ice layer were set to 200 nm. Since solid anisole remains transparent within this thickness range, we could easily locate the sample and selectively process specific areas without causing significant electron accumulation. Finally, a 2 keV electron beam was chosen for writing on solid anisole with thickness of 200 nm. It is worth noting that this condition results in

https://doi.org/10.1021/acs.nanolett.5c00378
Nano Lett. 2025, 25, 6168−6175

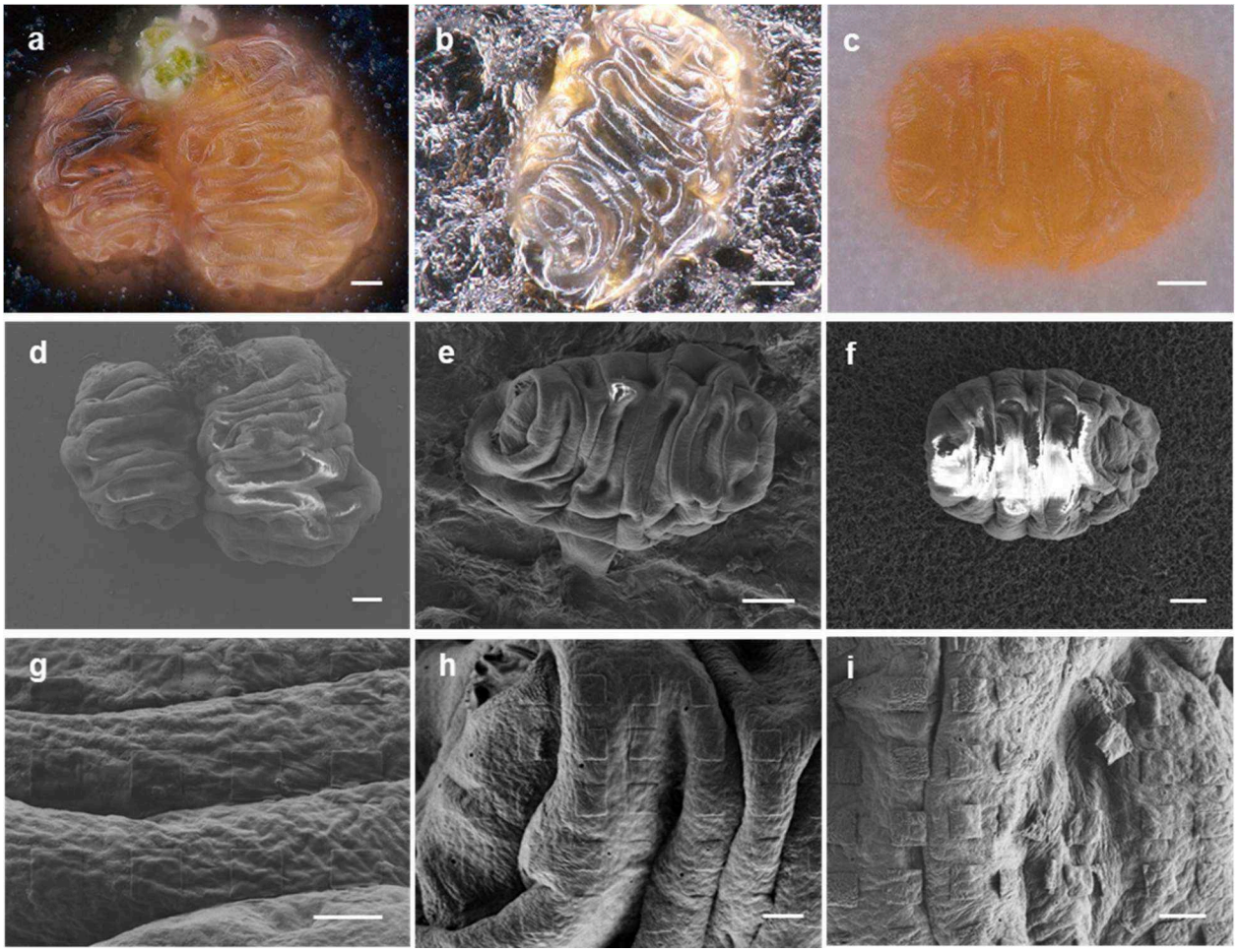

Figure 3. Comparison of tardigrades on different substrates: silicon wafer (a, d, and g), carbon nanocomposite paper (b, e, and h), and nylon microporous membrane (c, f, and i). Imaging includes 3D digital micrographs with large depth of field of tardigrades in their cryptobiotic state (a–c), SEM images acquired with the SE detector at an accelerating voltage of 2 keV (d–f), and fabricated square arrays with 3 μm side length and 3 μm spacing (g–i). Scale bars: 20 μm in (a)–(f) and 4 μm in (g)–(i).

unreacted anisole beneath cross-linked regions after e-beam exposure. Crucially, this residual anisole layer serves as a shielding barrier that attenuates electron penetration to the tardigrade, thereby significantly improving its viability. Such protective mechanisms would be particularly valuable when working with radiation-sensitive biological specimens. Moreover, low-energy beam patterning achieves reduced structural rigidity in fabricated architectures,[15] enabling closer conformity to the tardigrade's surface topography while mitigating the influence on its postrevival locomotion.

To achieve precise in situ patterning on live tardigrades, substrate selection should prioritize high electrical conductivity to minimize charge effects, high thermal conductivity for effective temperature control, and the ability to support tardigrades in transitioning to their cryptobiotic state. To identify the most suitable substrate, we evaluated silicon wafers, nylon microporous filters, and carbon nanocomposite paper. Tardigrades were induced into cryptobiosis on these substrates (Figures 3a–3c). The samples prepared on each substrate were then subjected to SEM observation (Figures 3d–3f) and ice lithography processing (Figures 3g–3i). Silicon wafers are commonly used in micro/nanofabrication due to their excellent electrical and thermal conductivity, however, their polished surfaces can cause rapid moisture loss, hindering tardigrades from entering cryptobiosis. Nylon microporous filters, resembling moss, create a favorable environment for tardigrades to enter cryptobiosis, resulting in a high survival rate. However, their poor electrical conductivity and electron beam-induced carbonization affect beam focusing and observation (Figure 3f). Additionally, their low thermal conductivity leads to uneven ice deposition, ultimately impacting the quality of the final processed patterns (Figure 3i). In contrast to the above substrates, carbon nanocomposite paper, which incorporates carbon nanotubes, graphene microsheets, and a small amount of resin, exhibits both good electrical and thermal conductivity. Furthermore, its loose and porous structure provides an ideal shelter for tardigrades, beneficial for their transition into the cryptobiotic state.

Finally, various patterns were successfully created onto tardigrades, including a nanowire array with an approximate line width of 72 nm (Figure 4a), microdisk arrays with a diameter and spacing of 3 μm (Figure 4b and Figure S4), square arrays with a side length and spacing of 3 μm (Figure 4c), and custom designs such as the Westlake University logo (Figure 4d). These patterns, resembling "tattoos," were carefully applied to the tardigrades. When conditions conducive to tardigrade activity were established, the tardigrades gradually absorbed water, expanded from their cryptobiotic state, extended their limbs, and ultimately regained vitality (Figure S5). To assess the pattern adhesion

https://doi.org/10.1021/acs.nanolett.5c00378
Nano Lett. 2025, 25, 6168–6175

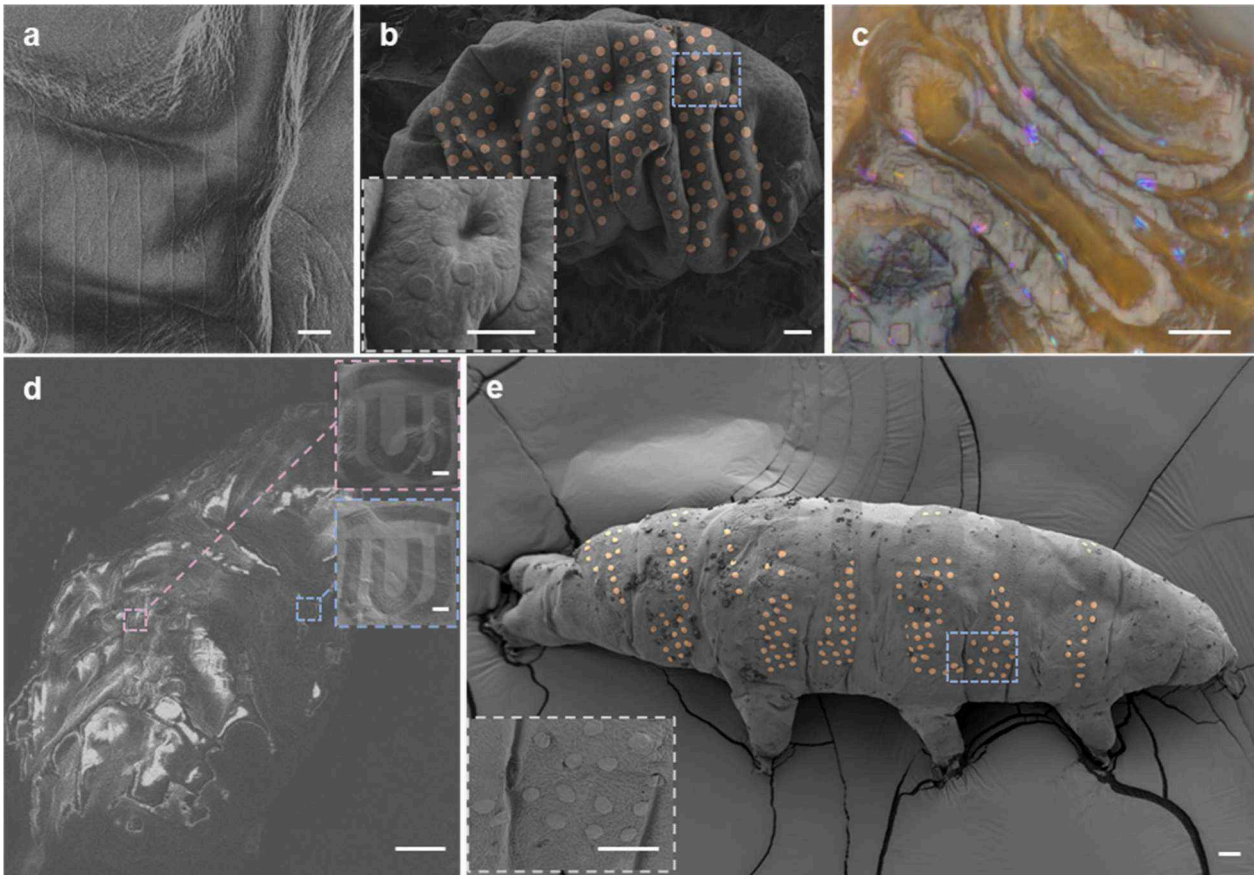

Figure 4. Microstructures created by ice lithography. (a) SEM image of nanolines on a tardigrade (~72 nm line width). (b) False-colored SEM image of a microdisk array (3 μm diameter, 3 μm spacing) on a tardigrade, with a magnified inset of the blue-boxed area. (c) 3D micrograph of a square array (3 μm side length, 3 μm spacing) on a tardigrade. (d) SEM image of the "Westlake University logo" array on a tardigrade. (e) False-colored SEM image of the tardigrade in (b) after rehydration and fixation, with a magnified inset of the blue-boxed area. Scale bars: 2 μm in (a), 20 μm in (d), 1 μm in inset of (d), and 10 μm in (b), (c), and (e).

and stability of the fabricated patterns on the tardigrades, as well as to visualize them clearly, fixation procedures were carried out approximately 5 h after rehydration. Moreover, in the 2 days after the tardigrade revived, we found the created pattern did not preclude the tardigrades from continuing to behave normally. The tardigrade with patterns could still enter a state of cryptobiosis, showing good biocompatibility of the patterning process. Figure 4e shows that the "tattoos" were well-preserved on the tardigrade's body, even after undergoing stretching, chemical exposure, rinsing, and drying. The magnified image provides a detailed view of the "tattoo" within the blue box. Additionally, focused ion beam (FIB) milling was employed to cut through the epidermis of tardigrades at sites where patterns were present. Cross-sectional analysis revealed that created patterns were closely connected with the tardigrade surface (Figure S6).

In our experiments, only one tardigrade was processed at a time, which can reduce the tardigrade's exposure time to vacuum and low temperatures. The e-beam exposure process requires different amounts of time depending on the pattern size, beam current, electron dose, and other parameters. If multiple samples are processed simultaneously, it results in prolonged exposure in the vacuum, which negatively impacts the survival rate of the tardigrades. After conducting dozens of experiments, we observed that the overall success rate for the revival of tardigrades was approximately 40%. However, this can be improved through better pretreatment to the tardigrades and optimization of the ice lithography process. The survival capability of tardigrades in extreme environments is closely related to their cryptobiosis state. By optimizing the conditions (including temperature, humidity, oxygen levels, and substrate) under which they transition from an active state to a cryptobiotic state, we can enhance their resistance and improve their revival rate after the experiment. Additionally, it is also beneficial to the revival of tardigrades by shortening the cooling time before e-beam exposure.

In summary, this study successfully demonstrates in situ fabrication of micro/nanopatterns on living organisms using ice lithography, including 72 nm-wide nanowires, array configurations, and arbitrary patterns at the micro/nanoscale. These patterns remain securely attached to the samples even after exposure to conditions such as stretching, soaking, rinsing, and drying. The tardigrades, along with the fabricated patterns, successfully revive when placed under suitable conditions. Additionally, we introduce an alternative substrate material, carbon nanocomposite paper, which shows significant promise for ice lithography applications. Although anisole was used as a precursor in this study, other chemicals such as alcohols, aromatics, alkanes, or organometallic compounds, could also be applied in ice lithography. By carefully selecting or combining different precursors, it is possible to fabricate structures with varied compositions and customized properties. For instance, metal patterns can be created on different parts of tardigrades' bodies using organometallic precursors. By

https://doi.org/10.1021/acs.nanolett.5c00378
Nano Lett. 2025, 25, 6168−6175

applying magnetic fields or targeted light exposure, we can precisely control their motion through magnetic interaction or photothermal effect, enabling to study their programmable, robot-like responses. This precise control also enables detailed investigations into tardigrade behavior (ethology) and movement patterns (kinematics), while also streamlining classification and rapid screening in experimental studies. In addition to tardigrades, our approach may also be applicable to other organisms with high stress resistance or those suitable for cryopreservation. We anticipate that the integration of more micro/nanofabrication techniques with biologically relevant systems at the micro/nanoscale will further advance fields such as microbial sensing, biomimetic devices, and living microrobots.

SAMPLE COLLECTION AND PREPARATION

Moss samples were collected in Hangzhou, China (sampling site coordinates: 30.236651, 120.164594). The samples were immersed in spring water for 10 h, followed by stirring. Afterward, sediment was collected using a sieve with a mesh size of approximately 100 μm. Tardigrades were then transferred under a stereo microscope (Nexcope, NSZ818) into growth medium. Spring water and the food was added to the dishes, which were then placed in a climate chamber set at 20 °C, 70% humidity, with a 12-h light/dark cycle.

Growth Medium. The Petri dishes were prepared by dissolving 1.2 g of agar powder in 100 mL of KCM solution (7 mg KCl, 8 mg CaCl, 8 mg $MgSO_4$, dissolved in 1 L of water). The mixture was shaken to ensure uniformity, then heated in a microwave oven on high for 3 min. The solution was poured into 35 mm Petri dishes, with a thickness of approximately 0.5 cm. After cooling, the dishes were stored in a refrigerator at 4 °C.

Food. The food used for feeding was Chlorococcum humicola, catalog number: FACHB-21, sourced from the Freshwater Algae Culture Collection at the Institute of Hydrobiology (FACHB), National Aquatic Biological Resource Center.

Desiccation-Induced Cryptobiosis. Tardigrades were transferred to precut 1 cm × 1 cm substrates and subjected to slow desiccation at 25 °C and 50% relative humidity for at least 5 days. After desiccation, the samples were stored in a drying oven for preservation.

MATERIALS AND ICE FORMATION

Anisole (99%) was procured from Macklin Biochemical (Shanghai, China) and used without further purification. Cooling of the sample was achieved in a SEM (Carl Zeiss, Sigma 300) chamber, which was evacuated and connected to an external liquid nitrogen dewar tank via a copper braid for efficient heat transfer. The sample, positioned on the cryostage, reached a stable temperature below 130 K. Anisole vapor, serving as the precursor, was introduced into the chamber through a controlled injection system. The inflow of vapor was regulated using a chamber valve, with the pressure drop monitored by a capacitive vacuum gauge (INFICON, Switzerland). By maintaining constant operational variables and controlling the pressure drop, the thickness of the ice layer was precisely managed. The ice thickness was estimated based on exposure to an electron beam exceeding the supersaturation dose and further validated using tapping-mode atomic force microscopy (AFM) topographic imaging (Oxford Instruments, Jupiter XR) after e-beam exposure.

E-BEAM EXPOSURE

Electron beam exposure was performed using a customized Carl Zeiss Sigma 300 scanning electron microscope (SEM). The SEM chamber was maintained at an ultrahigh vacuum pressure of 2×10^{-5} Pa, and an aperture size of 30 μm was utilized. During the exposure, an electron beam current of 50 pA was employed, and a step size of 0.012 μm was chosen. The dose used during exposure was 5 mC/cm^2. The dwell time was set to 1.667 μs, and a write field of 50 μm was defined for the exposure process.

SAMPLE FIXATION

Employing a micropipette, transfer the active state tardigrade into a culture dish. Anesthetize and immobilize it to an extended state by exposing them to a 60 °C water bath for 40 min. Prepare a 1% Triton solution with double-distilled water and immerse the anesthetized sample in the solution at 4 °C for 20 min. After a 30 min rinses in stationary liquid (2% PFA, 0.25% GA) and dehydrated through an ascending ethanol series (5 min each at 5%, 10%, 15%, 20%, 25%, 30%, 50%, 70%, 95%, 2 × absolute ethanol), transfer the tardigrade to a small filter paper bag. The small bag, containing the tardigrade, was then moved to absolute ethanol and subjected to a critical point dryer (Leica, EM CPD300). After the drying process, position the sample dorsal-up on carbon-conductive double-sided adhesive tape using tweezers. Subsequently, apply a 15 nm platinum (Pt) coating to the sample using a sputter coater (Leica, ACE600). Finally, observe the sample under an electron microscope.

CROSS-SECTIONAL IMAGING

Cross-sectional imaging was conducted with a ThermoFisher Helios 5 UX Focused Ion Beam Scanning Electron Microscope (FIB-SEM). To ensure sample preservation, the stage temperature was maintained at liquid nitrogen levels throughout the process. Prior to ion milling, a 200 nm thick layer of Pt was deposited on the sample to minimize potential damage and protect the surface during the milling procedure. Cross-sectional images were acquired by milling with gallium (Ga) ions. Imaging was conducted under the following conditions: acceleration voltage of 1 kV, beam current of 25 pA, and working distance of approximately 4 mm. The Through-Lens Detector (TLD) was used, with Secondary Electron (SE) imaging employed to capture the surface morphology.

SEM AND OPTICAL CHARACTERIZATION

SEM images were acquired using a ZEISS Sigma 300 Scanning Electron Microscope operating in high vacuum mode. The Secondary Electron (SE) detector was used for accurate observation. Imaging was conducted under the following conditions: acceleration voltage of 1 kV, beam current of 48 pA, aperture size of 30 μm, and working distance of 5.3 mm. Optical images were obtained with a ZEISS Axioscope 5 microscope.

https://doi.org/10.1021/acs.nanolett.5c00378
Nano Lett. 2025, 25, 6168−6175

■ ASSOCIATED CONTENT

Supporting Information

The Supporting Information is available free of charge at https://pubs.acs.org/doi/10.1021/acs.nanolett.5c00378.

SEM images of samples under different acceleration voltages; SEM images of samples under different detectors; Monte Carlo simulations of electron trajectories and absorbed energy in solid anisole films; microdisk arrays produced by ice lithography; dark-field optical images of the tardigrade with "tattoos" transitioning from a cryptobiotic state to an active state; and SEM images of cross-section at the solid anisole−tardigrade interface (PDF)

■ AUTHOR INFORMATION

Corresponding Authors

Ding Zhao − *Key Laboratory of 3D Micro/Nano Fabrication and Characterization of Zhejiang Province, School of Engineering, Westlake University, Hangzhou 310030, China; Westlake Institute for Optoelectronics, Hangzhou 311421, China;* orcid.org/0000-0001-9084-1521; Email: zhaoding@westlake.edu.cn

Min Qiu − *Key Laboratory of 3D Micro/Nano Fabrication and Characterization of Zhejiang Province, School of Engineering, Westlake University, Hangzhou 310030, China; Westlake Institute for Optoelectronics, Hangzhou 311421, China; Institute of Advanced Technology, Westlake Institute for Advanced Study, Hangzhou 310024, China;* orcid.org/0000-0002-4613-5125; Email: qiu_lab@westlake.edu.cn

Authors

Zhirong Yang − *Key Laboratory of 3D Micro/Nano Fabrication and Characterization of Zhejiang Province, School of Engineering, Westlake University, Hangzhou 310030, China;* orcid.org/0009-0005-5038-2187

Shan Wu − *Key Laboratory of 3D Micro/Nano Fabrication and Characterization of Zhejiang Province, School of Engineering, Westlake University, Hangzhou 310030, China*

Kang Zhao − *Westlake Institute for Optoelectronics, Hangzhou 311421, China*

Complete contact information is available at: https://pubs.acs.org/10.1021/acs.nanolett.5c00378

Author Contributions

D.Z. and M.Q. conceived the concept and supervised this research. Z.Y. and S.W. performed the experimental work on sample fabrication and characterization of nanostructures. Z.Y. and D.Z. conducted the visualization and validation of the data. Z.Y. and D.Z. wrote the manuscript with M.Q. All authors contributed to revisions and comments of the manuscript and discussed the results.

Funding

This project is supported by the National Natural Science Foundation of China (52203305, U21A20494, and 61927820).

Notes

The authors declare no competing financial interest.

■ ACKNOWLEDGMENTS

The authors express their sincere gratitude to Guicun Fang, Meng Shao, and their colleagues at the Biomedical Research Core Facilities of Westlake University for their invaluable assistance in obtaining and preparing the tardigrade samples.

■ REFERENCES

(1) Feynman, R. There's Plenty of Room at the Bottom: An Invitation to Enter a New Field of Physics. *Eng. Sci.* **1959**, *23* (5), 22−36.

(2) Wu, C.; Deng, H.; Huang, Y.-S.; Yu, H.; Takeuchi, I.; Rios Ocampo, C. A.; Li, M. Freeform Direct-Write and Rewritable Photonic Integrated Circuits in Phase-Change Thin Films. *Sci. Adv.* **2024**, *10* (1), No. eadk1361.

(3) Du, Y.; Shen, P.; Liu, H.; Zhang, Y.; Jia, L.; Pu, X.; Yang, F.; Ren, T.; Chu, D.; Wang, Z.; Wei, D. Multi-Receptor Skin with Highly Sensitive Tele-Perception Somatosensory. *Sci. Adv.* **2024**, *10* (37), No. eadp8681.

(4) Zheng, Q.; Peng, M.; Liu, Z.; Li, S.; Han, R.; Ouyang, H.; Fan, Y.; Pan, C.; Hu, W.; Zhai, J.; Li, Z.; Wang, Z. L. Dynamic Real-Time Imaging of Living Cell Traction Force by Piezo-Phototronic Light Nano-Antenna Array. *Sci. Adv.* **2021**, *7* (22), No. eabe7738.

(5) Grebenko, A. K.; Motovilov, K. A.; Bubis, A. V.; Nasibulin, A. G. Gentle Patterning Approaches toward Compatibility with Bio-Organic Materials and Their Environmental Aspects. *Small* **2022**, *18* (22), No. e2200476.

(6) Chen, Y. Applications of Nanoimprint Lithography/Hot Embossing: A Review. *Appl. Phys. A: Mater. Sci. Process.* **2015**, *121* (2), 451−465.

(7) Li, F.; Liu, S. F.; Liu, W.; Hou, Z. W.; Jiang, J.; Fu, Z.; Wang, S.; Si, Y.; Lu, S.; Zhou, H.; Liu, D.; Tian, X.; Qiu, H.; Yang, Y.; Li, Z.; Li, X.; Lin, L.; Sun, H. B.; Zhang, H.; Li, J. 3D Printing of Inorganic Nanomaterials by Photochemically Bonding Colloidal Nanocrystals. *Science* **2023**, *381* (6665), 1468−1474.

(8) McMullen, A.; Muñoz Basagoiti, M.; Zeravcic, Z.; Brujic, J. Self-Assembly of Emulsion Droplets Through Programmable Folding. *Nature* **2022**, *610* (7932), 502−506.

(9) Geng, J.; Xu, L.; Yan, W.; Shi, L.; Qiu, M. High-Speed Laser Writing of Structural Colors for Full-Color Inkless Printing. *Nat. Commun.* **2023**, *14* (1), 565.

(10) Di Marzio, N.; Eglin, D.; Serra, T.; Moroni, L. Bio-Fabrication: Convergence of 3D Bioprinting and Nano-Biomaterials in Tissue Engineering and Regenerative Medicine. *Front. Bioeng. Biotechnol.* **2020**, *8*, 326.

(11) Mannoor, M. S.; Jiang, Z.; James, T.; Kong, Y. L.; Malatesta, K. A.; Soboyejo, W. O.; Verma, N.; Gracias, D. H.; McAlpine, M. C. 3D Printed Bionic Ears. *Nano Lett.* **2013**, *13* (6), 2634−2639.

(12) Gahl, T. J.; Kunze, A. Force-Mediating Magnetic Nanoparticles to Engineer Neuronal Cell Function. *Front. Neurosci.* **2018**, *12*, 299.

(13) Mobjerg, N.; Neves, R. C. New Insights into Survival Strategies of Tardigrades. *Comp. Biochem. Physiol. A Mol. Integr. Physiol.* **2021**, *254*, No. 110890.

(14) Han, A.; Kuan, A.; Golovchenko, J.; Branton, D. Nano-patterning on Nonplanar and Fragile Substrates with Ice Resists. *Nano Lett.* **2012**, *12* (2), 1018−1021.

(15) Wu, S.; Zhao, D.; Qiu, M. 3D Nanoprinting by Electron-Beam with an Ice Resist. *ACS Appl. Mater. Interfaces* **2022**, *14* (1), 1652−1658.

(16) Yao, G.; Zhao, D.; Hong, Y.; Wu, S.; Liu, D.; Qiu, M. Direct Electron-Beam Patterning of Monolayer MoS_2 with Ice. *Nanoscale* **2020**, *12* (44), 22473−22477.

(17) Jin, B.; Zhao, D.; Liang, F.; Liu, L.; Liu, D.; Wang, P.; Qiu, M. Electron-Beam Irradiation Induced Regulation of Surface Defects in Lead Halide Perovskite Thin Films. *Research* **2021**, *2021*, No. 9797058.

(18) Murray, K. A.; Gibson, M. I. Chemical Approaches to Cryopreservation. *Nat. Rev. Chem.* **2022**, *6* (8), 579−593.

(19) Mobjerg, N.; Halberg, K. A.; Jorgensen, A.; Persson, D.; Bjorn, M.; Ramlov, H.; Kristensen, R. M. Survival in Extreme Environments - On the Current Knowledge of Adaptations in Tardigrades. *Acta Physiol.* **2011**, *202* (3), 409−420.

(20) Goldstein, B. Tardigrades and Their Emergence as Model Organisms. *Curr. Top. Dev. Biol.* **2022**, *147*, 173−198.
(21) Zhao, D.; Han, A.; Qiu, M. Ice Lithography for 3D Nanofabrication. *Sci. Bull.* **2019**, *64* (12), 865−871.
(22) Hong, Y.; Zhao, D.; Wang, J.; Lu, J.; Yao, G.; Liu, D.; Luo, H.; Li, Q.; Qiu, M. Solvent-Free Nanofabrication Based on Ice-Assisted Electron-Beam Lithography. *Nano Lett.* **2020**, *20* (12), 8841−8846.
(23) Jin, B.; Hong, Y.; Li, Z.; Zhao, D.; Lu, Y.; Yao, G.; Zheng, R.; Bi, G.; Zhang, Q.; Fang, X.; Qiu, M. Ice-Assisted Electron-Beam Lithography for Halide Perovskite Optoelectronic Nanodevices. *Nano Energy* **2022**, *102*, No. 107692.
(24) Hong, Y.; Zhao, D.; Liu, D.; Yao, G.; Qiu, M. Development of an In-Situ Nanofabrication Instrument for Ice Lithography. *Microelectron. Eng.* **2020**, *224*, No. 111251.
(25) Lu, Y.; Jin, B.; Zheng, R.; Wu, S.; Zhao, D.; Qiu, M. Production and Patterning of Fluorescent Quantum Dots by Cryogenic Electron-Beam Writing. *ACS Appl. Mater. Interfaces* **2023**, *15* (9), 12154−12160.

https://doi.org/10.1021/acs.nanolett.5c00378
Nano Lett. 2025, 25, 6168−6175

Supporting Information

Patterning on Living Tardigrades

Zhirong Yang[1], Shan Wu[1], Kang Zhao[2], Ding Zhao[1,2], Min Qiu[1,2,3]**

[1] Key Laboratory of 3D Micro/Nano Fabrication and Characterization of Zhejiang Province, School of Engineering, Westlake University, Hangzhou 310030, China

[2] Westlake Institute for Optoelectronics, Fuyang, Hangzhou 311421, China

[3] Institute of Advanced Technology, Westlake Institute for Advanced Study, Hangzhou 310024, China.

Corresponding author: zhaoding@westlake.edu.cn (D.Z.), qiu_lab@westlake.edu.cn (M.Q.)

This file includes:

Figures S1 to S6.

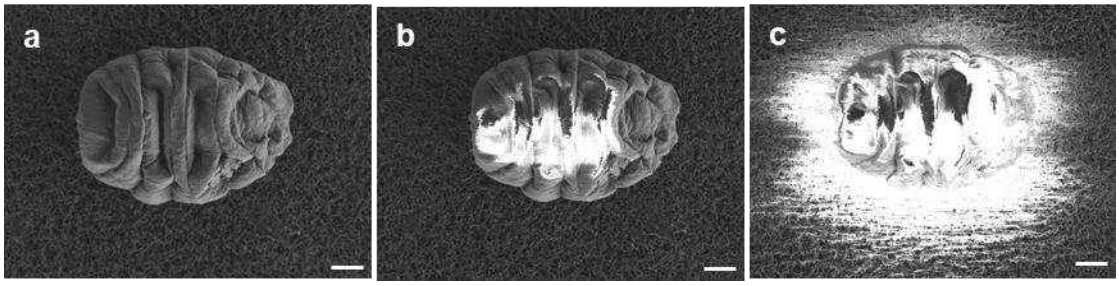

Figure S1. SEM images of tardigrades at accelerating voltages of 1 keV (a), 2 keV (b), and 3 keV (c). Scale bars: 20 μm.

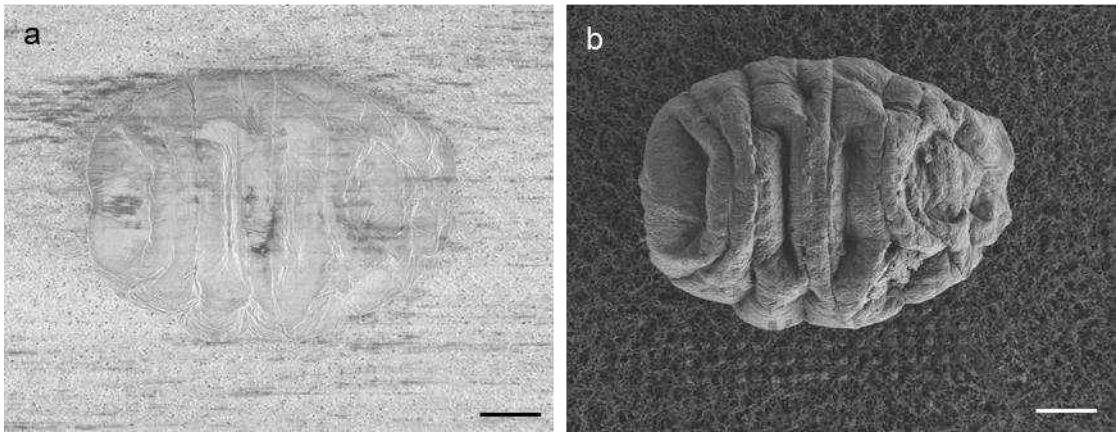

Figure S2. SEM images of the tardigrade with patterns obtained using different detectors: (a) Inlens detector and (b) SE detector. Scanning electron microscope model: Zeiss Sigma 300. Observation conditions: 1 kV voltage, 48 pA beam current, 30 μm aperture size, and a working distance of 5.3 mm. Scale bars: 20 μm.

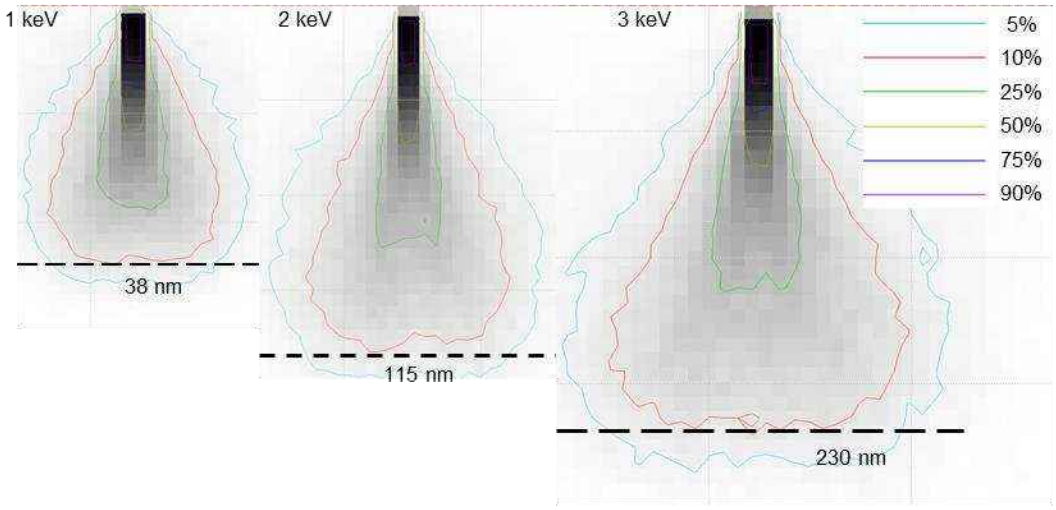

Figure S3. Monte Carlo simulations of electron trajectories and absorbed energy in solid anisole films at 1 keV, 2 keV, and 3 keV. The number of electrons was 10000. The physical model was set as Mott by interpolation.

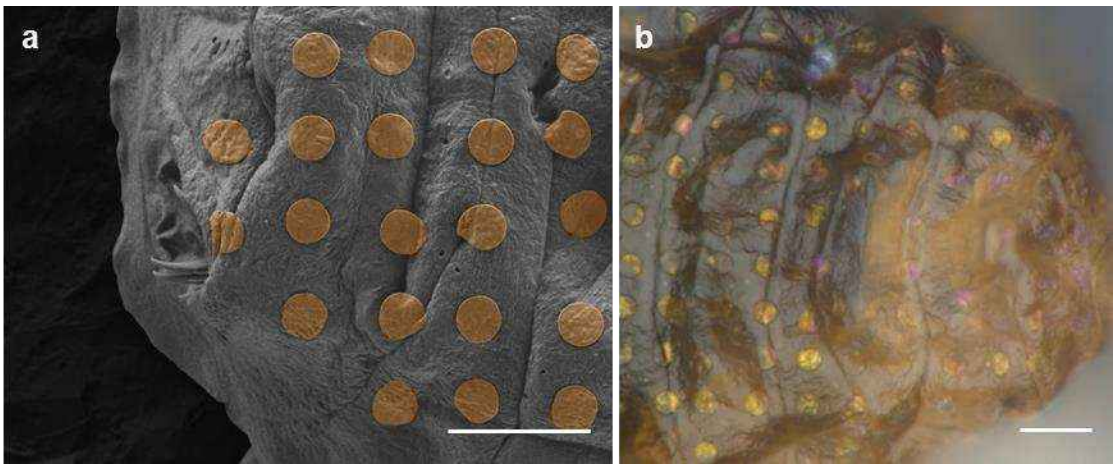

Figure S4. Microdisk arrays produced by ice lithography. (a) False-colored SEM image and (b) corresponding optical image of the same tardigrade post-patterning, featuring circles with a diameter of 3 µm and a spacing of 3 µm. For e-beam patterning, the beam current is 0.05 nA and the electron dose is 5 mC/cm² at 3kV. Scale bars: 10 µm.

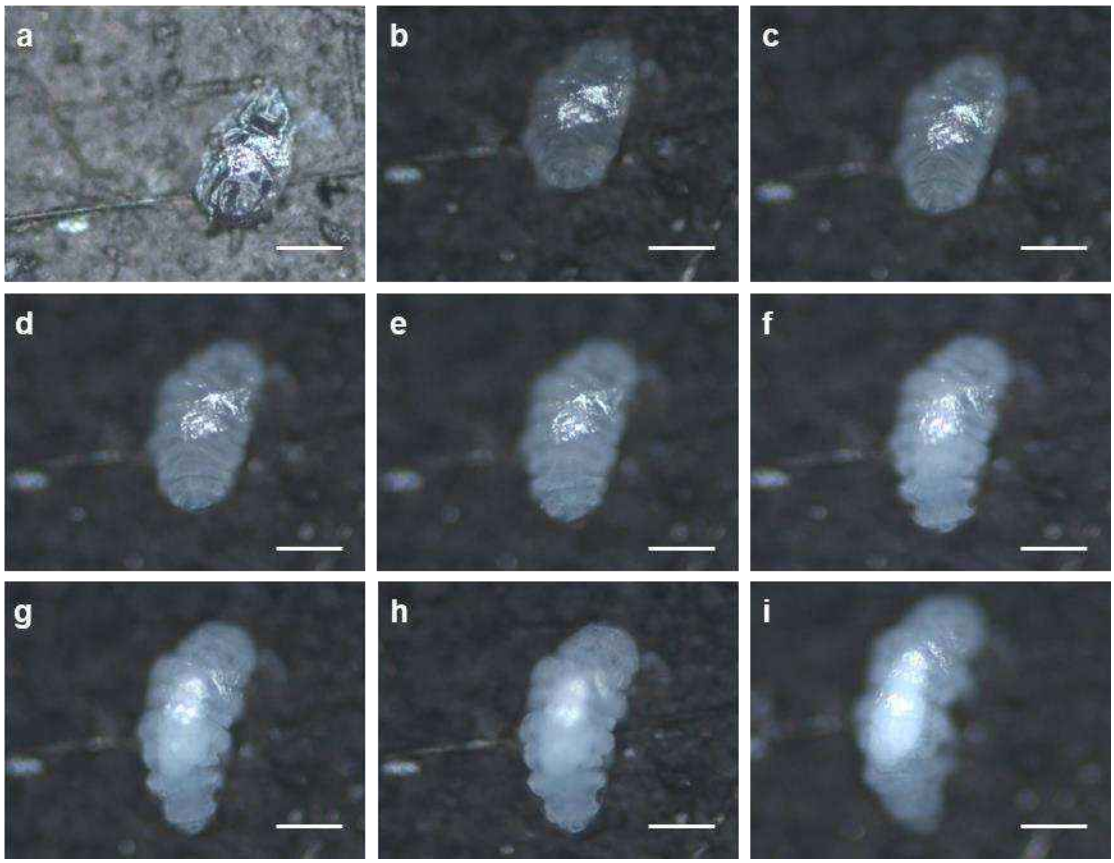

Figure S5. Dark-field optical images of the tardigrade with "tattoos" transitioning from a cryptobiotic state to an active state. Time interval between captured images is approximately two minutes. Scale bars: 100 µm.

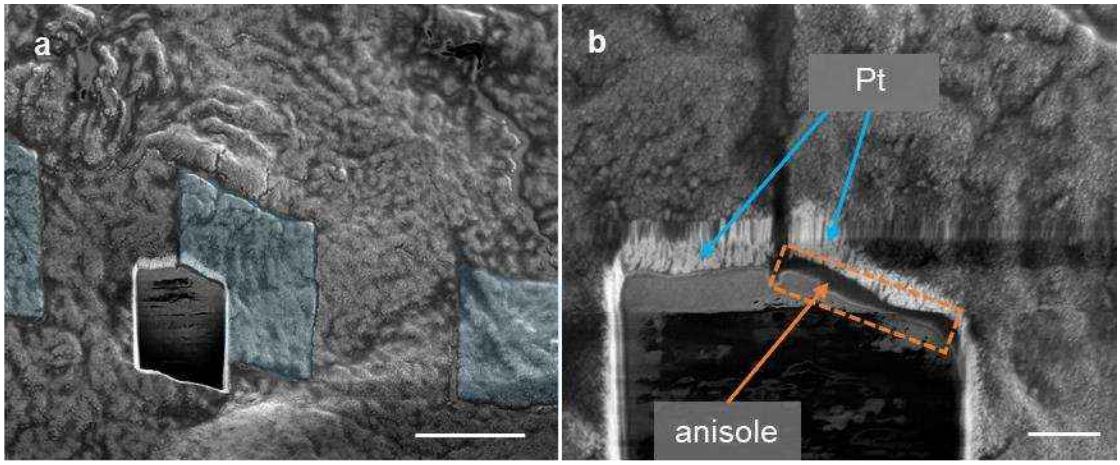

Figure S6. SEM images of cross-section at the exposed solid anisole–tardigrade interface. (a) SEM image of the square pattern (blue areas) fabricated on a tardigrade, with a cross-sectional view at the exposed solid anisole–tardigrade interface obtained by milling the pattern. The sample was tilted at 53° during observation, and pre-coated with 200 nm of Pt to minimize damage to the anisole structure. (b) Magnified view of the cross-sectional area, with the exposed solid anisole and platinum coating indicated by orange and blue arrows, respectively. Scale bars: 3 μm in (a); 500 nm in (b).